Crystal Chemistry of the 4,4′-Dimethyl-2,2′bipyridine/Copper Bromide System

Roger D. Willett,* George Pon, and Callie Nagy

Department of Chemistry, Washington State University, Pullman, Washington 99164

Received February 27, 2001

The reaction of 4,4′-dimethyl-2,2-bipyridine (henceforth dmbp) with copper(I) and/or copper(II) bromide under a wide variety of conditions has led to the isolation of 10 different crystalline materials. These include one Cu(I) salt, $[Cu(dmbp)_2]Br$ (a distorted tetrahedral Cu species and a lattice Br^- ion); two mixed valence Cu(I,II) compounds, $[Cu(dmbp)_2Br][CuBr_2]$ (discrete 5-coordinated Cu(II) and linear Cu(I) species) and $Cu(dmbp)_2BrCu_2Br_3$ (linked 5-coordinate Cu(II) and trigonal planar Cu(I) species); and seven Cu(II) compounds, $(dmbp)CuBr_2$ (stacked planar monomers), $[(dmbp)CuBr_2]_2$(five coordinate bibridged dimers), $(dmbp)Cu_2Br_4$ (stacked planar bibridged dimers), $(dmbp)CuBr_2$(DMSO) (five coordinate monomers), $[Cu(dmbp)_2Br]OH\cdot5^1/_2H_2O$ and $[Cu(dmbp)_2Br](Br/OH)\cdot5^1/_2H_2O$ (five coordinate monomers), and $(dmbpH_2)CuBr_4\cdot H_2O$ (distorted tetrahedral monomers). The crystal structure determinations of these materials are reported. A common thread in their structural chemistry is the supramolecular architecture developed through interdigitation of the dmbp rings on neighboring molecular species. The interdigitation leads to layer structures in many of the materials. The distances between the interdigitated dmbp rings are in the range 3.4−3.7 Å. The $Cu(dmbp)_2Br^+$ species exhibits an exceptionally large distortion from tetrahedral geometry due to deviation of the dihedral angle between the mean planes of the Cu(dmbp) fragments from 90°. The $Cu(dmbp)_2Br^+$ cations have distorted trigonal bipyramidal geometry, the Br^- ion occupying an equatorial position. The length of the Cu−Br bond in the $Cu(dmbp)_2Br^+$ species is correlated with the change in dihedral angle between the planes of the two dmbp ligands. The mono-dmbp complexes show a greater variation in coordination geometry for the Cu(II) species, including distorted trigonal bipyramidal and augmented square planar 4 + 1 and 4 + 2 coordination.

Introduction

Metal ion complexes with bidentate ligands continue to be of strong interest in many areas of chemistry. Ligands based on the 2,2′-bipyridine (bpy) and the *o*-phenanthroline frameworks have played a particularly important role because of the imbedded π electron system present. Their complexes with metal ions spanning much of the periodic table have led to a wide variety of systems with interesting structural, spectroscopic, catalytic, biomimetic, etc. properties.[1] Copper complexes have been studied for a variety of reasons, including interest in their properties as catalysts in organic synthesis and in control of polymerization reactions, etc.[2] Other recent studies of Cu(II) with *o*-phenanthroline type ligands have focused, for example, on the effect of substituents on the ground state as well as excited-state distortions and on redox behavior.[3] Our laboratory has had a strong interest in the stereochemistry and structural chemistry of copper(II) halide complexes and in the characterization of their thermal and magnetic properties.[4] In the course of the synthesis of these compounds, we have observed frequent incidents of autoredox processes, particularly when the halide is bromide. This has led to an interest in the preparation of mixed valence Cu(I)/Cu(II) halide complexes and in the crystal engineering of extended Cu(I) halide lattices.[5]

In 1999, Hammond et al. reported an investigation of the hydrothermal synthesis of a variety of materials in the Cu(I)/Cu(II)/Br/bpy system.[2f] This included both Cu(I) and Cu(II) species, as well as the existence of a mixed valence Cu(I/II)

(1) (a) Otsuka, T.; Takahashi, N.; Fujigasaki, N.; Sekine, A.; Ohashi, Y.; Kaizu, Y. *Inorg. Chem.* **1999**, *38*, 1340. (b) Wada, T.; Tsuge, K.; Tanaka, K. *Inorg. Chem.* **2000**, *39*, 1340 (c) Sjodin, M.; Styring, S.; Akermark, B.; Sun, L.; Hammarstrom, L. *J. Am. Chem. Soc.* **2000**, *122*, 3932. (d) Gao, F. G.; Bard, A. J. *J. Am. Chem. Soc.* **2000**, *12*, 7426. (e) Alsfasser, R.; van Eldik, R. *Inorg. Chem.* **1996**, *35*, 628. (f) Real, J. A.; Munoz, M. C.; Faus, J.; Solans, X. *Inorg. Chem.* **1997**, *36*, 3008. (g) Garribba, E.; Micera, G.; Sanna-Erre, D. *Inorg. Chim. Acta* **2000**, *299*, 253. (h) Guo, J.; Han, Z.; Wu. P. *J. Mol. Catal. A* **2000**, *159*, 77.

(2) (a) Emmenegger, F.; Williams, M. E.; Murray, R. W. *Inorg. Chem.* **1997**, *36*, 3146. (b) Matyjaszewski, K.; Patten, T.; Xia, J. *J. Am. Chem. Soc.* **1997**, *119*, 674. (c) Kickelbick, G.; Reinohl, U.; Ertel, T. S.; Weber, A.; Bertagnolli, H.; Matyjaszewski, K. *Inorg. Chem.* **2001**, *40*, 6. (d) Levy, A. M.; Olmstead, M. M.; Patten, T. E. *Inorg. Chem.* **2000**, *39*, 1628. (e) Menon, S.; Rajasekharan, M. V.; Tuchagues, J.-P. *Inorg. Chem.* **1997**, *36*, 4341. (f) Hammond, R. P.; Cavaluzzi, M.; Haushalter, R. C. Zubieta, J. A. *Inorg. Chem.* **1999**, *38*, 1288. (h) Hammond, R. P.; Chesnut, D. J.; Zubieta, J. A. *J. Solid State Chem.* **2001**, *158*, 55. (i) Skelton, B. W.; Waters, A. F.; White, A. H. *Aust. J. Chem.* **1991**, *44*, 1207.

(3) (a) Miller, M. T.; Gantzel, P. K.; Karpishin, T. B. *Inorg. Chem.* **1998**, *37*, 2285. (b) Murphy, G.; O'Sullivan, C.; Murphy, B.; Hathaway, B. *Inorg. Chem.* **1998**, *37*, 240. (c) Burs, P. M.; Whitehead, J. P.; Pink, C. C.; Gramm, E. C.; Eglin, J. L.; Watton, S. P.; Pence, L. E. *Inorg. Chem.* **2001**, *40*, 1871.

(4) (a) Geiser, U.; Willett, R. D. *Acta Chem. Crot.* **1984**, *57*, 751. (b) Geiser, U.; Willett, R. D.; Lindbeck, M.; Emerson, K. *J. Am. Chem. Soc.* **1986**, *108*, 1173. (c) Wei, M.; Willett, R. D.; Atanasov, M. *Z. Phys. Chem.* **1997**, *200*, 31. (d) Weiss, S.; Willett, R. D. *Acta Crystallogr.* **1993**, *B49*, 283. (e) Willett, R. D. *Acta Crystallogr.* **1993**, *A49*, 613. (g) Scott, B.; Willett, R. D. *J. Am. Chem. Soc.* **1991**, *113*, 5253. (h) Willett, R. D. *Coord. Chem. Rev.* **1991**, *109*, 181. (i) Bond, M. R.; Willett, R. D.; Rubenacker, G. V. *Inorg. Chem.* **1990**, *29*, 2713. (j) Bond, M. R.; Willett, R. D. *Inorg. Chem.* **1989**, *28*, 893. (k) Place, H.; Willett, R. D. *Acta Crystallogr.* **1988**, *C43*, 34.

(5) (a) Scott, B.; Willett, R. D.; Porter, L.; Williams, J. *Inorg. Chem.* **1992**, *31*, 2483. (b) Willett, R. D. *Inorg. Chem.* **1987**, *26*, 3423. (c) Willett, R. D.; West, D. X. *Acta Crystallogr.* **1987**, *C43*, 2300. (d) Willett, R. D.; Halvorson, K. *Acta Crystallogr.* **1988**, *C44*, 2068. (e) Willett, R. D.; Vij, A. *J. Chem. Crystallogr.* **2001**, *30*, 399. (f) Willett, R. D. *Inorg. Chem.* **2001**, *40*, 966. (g) Place, H.; Scott, B.; Long, G.; Willett, R. D. *Inorg. Chim. Acta* **1998**, *279*, 1.

10.1021/ic010229v CCC: $20.00
Published on Web 07/10/2001

species. One of the observed structures involved a one-dimensional polymer based on the aggregation of planar four coordinate Cu(II)(pby)Br_2 species. Here the coordination sphere of the copper(II) ion is augmented by two longer semicoordinate Cu−Br bonds in the formation of the polymeric chain structure. A second reported structure contained a mixed valence system of Cu(II)$(bpy)_2Br^+$ monomers linked to $Cu(I)_4Br_6^{2-}$ oligomers via Cu(II)−Br−Cu(I) bridges. In this system, the five-coordinate copper(II) ion has a distorted trigonal bipyramidal geometry while the anionic oligomer has copper(I) ions with either a trigonal planar geometry or a tetrahedral geometry. In a more recent report[2g] of their study of the Cu(I)/Cu(II)/en system (en = ethylenediamine), the authors reported two mixed valence systems: Cu(en)Cu_2Br_4 and Cu(en)Cu_5Br_7. Both contain Cu(I) bromide chains stabilized by the formation of semicoordinate bonds between the $Cu(en)_2^{2+}$ species and halide ions associated with the Cu(I) bromide chain. In the former case, the chains consist of face-shared $CuBr_4$ tetrahedra, while in the latter the chains are formed by the formation of Cu−Br bridges between pentagonal bipyramidal $Cu_5Br_7^{2-}$ oligomers. On the other hand, because of their importance as polymerization catalysts, Levy et al have recently looked at the structure of one of the products of the reactions of 4,4′-substituted bipyridines with CuBr.[2d] They obtained a salt that contained a distorted tetrahedral $Cu(sbpy)_2^+$ cation and a linear $CuBr_2^-$ anion (sbpy = substituted bpy). Another structural type for Cu(I)/sbpy complexes is the μ_2-Br dimer as observed by Skelton et al. in $Cu_2Br_2(bpy)_2$,[2h] where the $CuBr_2N_2$ coordination sphere has a distorted tetrahedral geometry. These examples represent the typical coordination geometries observed for copper(I) and copper(II) species in bipyridine type complexes.

Our interest in bipyridine-based systems has focused on 4,4′-dimethyl-2,2′-bipyridine (henceforth dmbp) complexes, following our synthesis of the novel dimer complexes (dmbp)Cu_2X_4 (X = Cl, Br).[6] During our initial investigation, several different complexes were isolated, in addition to the (dmbp)Cu_2X_4 complexes. Following the publication of Hammond et al.[2f] of their study of the bpy system, we decided to further investigate the dmbp system, with the hope of isolating new mixed valence or Cu(I) halide systems. In this paper we report the results of our crystal chemistry study of the system, which resulted in the isolation of 10 different crystalline substances.

Experimental Section

Synthesis. Initial synthetic strategies simply involved the crystallization by slow evaporation of aqueous containing varying molar ratios of $CuBr_2$ and dmbp. The $CuBr_2$/dmbp ratios were varied between 1:1 to 3:1. A small amount of HBr was added to the solution to retard hydrolysis of Cu(II). In one case, crystallization from concentrated HBr solution was carried out while, in another case, DMSO was used as a solvent. Following the report of Hammond et al.,[2f] a modification of their procedure was used to attempt to further explore the crystal chemistry of this system. To reduce the risk of air oxidation for the Cu(I) salt and the mixed valence Cu(I/II) materials, excess solid materials were placed in a small test tube in a hot mineral oil bath at 90 °C and hot water was added. The tube was then sealed with a rubber septum. The tubes were held at that temperature for 24 h and then allowed to cool to room temperature. A wide variety of ratios of CuBr, $CuBr_2$, CuO, and dmbp were used, similar to the ratios utilized by Hammond et al. The solid materials were separated and crystals selected for diffraction studies.

Starting Materials. $CuBr_2$(Baker), CuBr(Aldrich), CuO(Baker), dmbp (Aldrich), DMSO(Fisher) and HBr (Fisher) were used without further purification.

(a) [Cu(dmbp)$_2$]Br (1). A mixture of 0.5 mmol CuBr, 1.0 mmol dmbp, and 4 mL water were placed in a closed test tube and held at 90 °C for 24 h. After cooling to room temperature, the solid material was filtered off. It consisted primarily of reddish-orange platelets. A crystal of dimensions 0.4 × 0.2 × 0.05 mm was selected for X-ray analysis. The compound is triclinic, space group $P\bar{1}$, with a = 7.671(2), b = 11.478(3), c = 13.808(3) Å, α = 95.01(2), β = 100.92, and γ = 109.09° with Z = 2.

(b) Cu[(dmbp)$_2$Br](OH) ·5^1/$_2$H$_2$O (2). A 1:1:1.6 mole ratio mixture of CuBr, $CuBr_2$, dmbp was dissolved in 40 mL of water in a 50 mL beaker. The solution was slowly evaporated until near dryness, at which time thin green slats had crystallized. A crystal with area of 0.5 × 0.2 mm and a thickness of less than 0.02 mm was used for the data collection. The apparent space group for the monoclinic lattice is $P2/c$ with a = 51.952(10), b = 7.775(2), c = 14.098(3) Å, and β = 105.67-(3)° with Z = 8.

(c) [Cu(dmbp)$_2$Br](Br/OH)·5^1/$_2$H$_2$O (2′) and [Cu(dmbp)$_2$Br]-[CuBr$_2$] (3). A mixture of 0.5 mmol CuBr, 0.5 mmol $CuBr_2$, 0.8 mmol dmbp, and 2 mL water were place in a closed test tube held at 90 °C for 24 h. After cooling to room temperature, the solid material consisted of pleochroic crystals of **2′**, reddish-orange crystals of **1** and green rods of **3**. A thin slat of **2′** with dimensions 0.5 × 0.2 mm and less than 0.02 mm thick was selected for X-ray analysis. The structure is monoclinic, $P2/c$, with a =13.390(3), b = 7.487(2), c = 14.449(3) Å, and β = 105.85(3)° with Z = 2. For **3**, a green, nearly opaque crystal of dimensions 0.3 × 0.3 × 0.1 mm was selected and analysis gave a triclinic cell, space group $P\bar{1}$, with a = 8.8329(5), b = 11.2819(6), c = 14.0647(7) Å, α = 99.956(2), β = 100.252(2), and γ = 94.901(2)° with Z = 2.

(d) Cu(dmbp)$_2$BrCu$_2$Br$_3$ (4). A mixture of 0.5 mmol CuBr, 0.5 mmol $CuBr_2$, 0.05 mmol CuO, 0.8 mmol dmbp, and 2 mL water were place in a closed test tube held at 90 °C for 24 h. After cooling to room temperature, the solid material consisted of opaque needles of **4**, in addition to smaller amounts of crystals identified as **1**, **2**, and **6**. A crystal with dimensions 0.2 × 0.075 × 0.075 mm was used for the X-ray study. This compound is also triclinic, space group $P\bar{1}$, with a = 8.5021(3), b = 10.8577(4), c = 15.591(1) Å, α = 89.116(2), β = 82.644(2), and γ = 79.418(2)° with Z = 2.

(e) [(dmbp)CuBr$_2$]$_2$ (5). Evaporation of a 1:1 mixture of $CuBr_2$ and dmbp dissolved in water at 90 °C yielded thin purple plates. A brown, nearly opaque crystal 0.6 × 0.1 × 0.02 mm also gave a triclinic unit cell with space group $P\bar{1}$, with a = 7.4524(3), b = 9.6154(3), c = 11.5976(1) Å, α = 107.821(2), β = 97.491(2), and γ = 112.248(2)° with Z = 2.

(f) (dmbp)CuBr$_2$ (6). Evaporation of a 1:1 mixture (0.10 mol) of $CuBr_2$ and dmbp dissolved in 50 mL of water acidified with a small amount of concentrated HBr at room temperature yielded pleochroic needles. A crystal 0.3 × 0.2 × 0.15 mm was chosen and yielded a monoclinic space group, $C2/c$, with a = 18.32(4), b = 9.817(2), c = 7.483(2) Å, and β = 107.86(3)° with Z = 4.

(g) (dmbp)Cu$_2$Br$_4$ (7). Evaporation of 50 mL of acidified aqueous solution containing a 2:1 ratio (0.20 and 0.10 mol) of $CuBr_2$ to dmbp at room temperature yielded purple multifaceted crystals. A purple crystal 0.4 × 0.2 × 0.15 mm was chosen and yielded a monoclinic space group, $C2/c$, with a = 17.3718(5), b = 13.3189(1), c = 7.4432-(2) Å, and β = 110.686(2)° with Z = 4.

(h) (dmbp)CuBr$_2$(DMSO) (8). Crystallization of an equimolar mixture of $CuBr_2$ and dmbp (0.10 mol) from 50 mL DMSO acidified with a few drops of concentrated HBr yielded green crystals. A small crystal of dimensions of approximately 0.1 × 0.2 × 0.2 mm was selected for X-ray analysis. The structure is monoclinic space group, $P2_1/c$, with a = 8.142(1), b = 15.395(3), c = 14.472(2) Å, and β = 103.21(1)° with Z = 4.

(i) (dmbpH$_2$)CuBr$_4$·H$_2$O (9). Evaporation of a 1:1 mixture (0.10 mol) of $CuBr_2$ and dmbp dissolved in 30 mL concentrated (18 M) HBr at room temperature yielded purple platelets. A sample with dimensions roughly 0.2 × 0.4 × 0.4 mm was chosen for X-ray work. The analysis yielded a monoclinic space group, $P2_1/c$, with a = 7.930(2), b = 12.645-(2), c = 18.494(3) Å, and β = 102.40(2)° with Z = 4.

The varying conditions under which the reactions were carried out have lead to the formation of compounds with various Cu(I)/Cu(II)/

(6) Willett, R. D.; Bond, M. R.; Pon, G. *Inorg. Chem.* **1990**, *29*, 4160.

Table 1. Crystallographic Data for Compounds **1**−**4** and **5**−**9**

	1	**2**	**2′**	**3**	**4**
chem formula	$C_{24}H_{24}N_4CuBr$	$C_{24}H_{37}N_4O_{6.5}CuBr$	$C_{24}H_{35.1}N_4O_{5.6}CuBr_{1.9}$	$C_{24}H_{24}N_4Cu_2Br_3$	$C_{24}H_{24}N_4Cu_3Br_4$
a, Å	7.671(2)	51.982(10)	13.390(3)	8.8329(5)	8.5021(3)
b, Å	11.478(3)	7.275(2)	7.487(2)	11.2819(6)	10.8577(4)
c, Å	13.808(3)	14.098(3)	14.449(3)	14.0647	15.5912(1)
α, deg	95.01(2)	90	90	99.956(2)	89.116(2)
β, deg	100.92(2)	105.67(3)	105.85(3)	100.252(2)	82.644(2)
γ, deg	109.09(2)	90	90	94.90(2)	79.418(2)
V, Å^3	1113.3(4)	5133(2)	1393.5(5)	1348.63(12)	1403.10(7)
Z	2	8	2	2	2
fw	255.96	628.02	687.15	735.28	878.73
space group	$P\bar{1}$	$P2/c$	$P2/c$	$P\bar{1}$	$P\bar{1}$
T, K	298	298	298	298	298
λ, Å	0.71073	0.71073	0.71073	0.71073	0.71073
D_{calc}, g cm^{-3}	1.527	1.625	1.638	1.811	2.080
μ, mm^{-1}	2.793	2.46	3.61	6.040	7.969
R1[a]	0.0472/0.0595	0.124/0.180	0.0588/0.0745	0.0736/0.0970	0.106/0.155
wR2[b]	0.0916/0.0989	0.316/0.359	0.138/0.148	0.141/0.154	0.206/0.241

	5	**6**	**7**	**8**	**9**
chem formula	$C_{24}H_{24}N_4Cu_2Br_4$	$C_{12}H_{12}N_2CuBr_2$	$C_{12}H_{12}N_2Cu_2Br_4$	$C_{14}H_{18}N_2OSCuBr_2$	$C_{12}H_{16}N_2OCuBr_4$
a, Å	7.4524(3)	18.320(4)	17.3718(5)	8.142(1)	7.930(2)
b, Å	9.6154(3)	9.817(2)	13.3189(1)	15.395(3)	12.645(2)
c, Å	11.5976(1)	7.483(2)	7.4432(2)	14.472(2)	18.494(3)
α, deg	107.821(2)	90	90	90	90
β, deg	97.491(2)	107.86(3)	110.686(2)	103.21(1)	102.40(2)
γ, deg	112.248(2)	90	90	90	90
V, Å^3	703.10(4)	1281.0(4)	1611.13(6)	1766.1(5)	1811.1(6)
Z	1	4	4	4	4
fw	815.19	407.60	632.96	485.76	587.48
space group	$P\bar{1}$	$C2/c$	$C2/c$	$P2_1/c$	$P2_1/c$
T, K	298	298	298	298	298
λ, Å	0.71073	0.71069	0.71069	0.71069	0.71069
D_{calc}, g cm^{-3}	1.925	2.113	2.61	1.83	2.15
μ, mm^{-1}	7.22	7.92	12.55	58.4	99.5
R1	0.142/0.185	0.0293/0.0359	0.0560/0.1777	0.0490/	0.0463
wR2	0.358/0.401	0.676/0.0704	0.129/0.1578	0.0334/	0.0501

[a] $R1 = \sum||F_o| - |F_c||/\sum|F_o|^2$. [b] $wR2 = \{\sum[w(F_o^2 - F_c^2)^2/\sum[w(F_c^2)^2]\}^{1/2}$.

Scheme 1

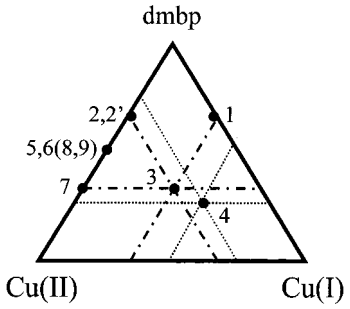

dmbp ratios. Given the nature of the coordination chemistry of both the Cu(I) and the Cu(II) ions, the redox active nature of the cu/Br system, and the bridging capabilities of the Br^- anions, it is unlikely that all possible crystalline materials have been isolated, particularly if more extreme thermal conditions were to be employed. The variation in composition of the compounds obtained can be best represented by construction of a three component phase diagram (Scheme 1). The ratio of dmbp to total copper is 2:1 for the Cu(I) salt, **1**, and two hydrated Cu(II) systems, **2** and **2′**. The ratio is 1:1 for the Cu(II) polymorphs **5** and **6** (as well as for **8** and **9**, obtained from DMSO and concentrated HBr solutions respectively). The ratio drops to 1:2 for the Cu(II) dimer system, **7**, and for the ionic mixed valence salt, **3**. Finally, the molecular mixed valence compound, **4**, has a 1:3 dmbp/total Cu ratio.

X-ray Diffraction. Data for compounds **1**−**7** were collected on a Bruker 3-circle platform diffractometer equipped with a CCD detector. The frame data were acquired with the SMART[7] software at 295 K using Mo Kα radiation ($\lambda = 0.71073$ Å) from a fine-focus tube. Final values of the cell parameters were obtained from least squares refinement of the positions of all observed reflections. A total of 1271 frames were collected in three sets and a final set of 50 frames, identical to the first 50 frames, was also collected to determine crystal decay. The data were processed using the SAINT software.[8] Absorption corrections were performed using the SADABS[9] program. The structures were solved by direct methods or Patterson techniques using the SHELX-90[10] program and refined by least-squares method on F^2, SHELXL-93,[11] incorporated in SHELXTL V 5.03.[12] Hydrogen atoms for the dmbp ligands were generally found on the difference Fourier maps, except for the methyl protons. For the cases where the protons were located, their positional and thermal parameters were usually refined. When not located, they were included at calculated positions. Hydrogen atoms for the lattice water molecules in **2** and **2′** were not included, for the reasons discussed below.

X-ray diffraction data for compounds **8** and **9** were collected with a Syntex $P2_1$ diffractometer, upgraded to Siemens P3 specifications, and equipped with a graphite monochromator. Lattice constants were obtained from 25 accurately centered high angle ($27° \le 2\theta \le 35°$) reflections. Data were collected out to $2\theta = 45°$ and those with $|F_o| \ge 3\sigma(F)$ retained for structure analysis.[13] Data were corrected for absorption utilizing psi scan data assuming an ellipsoidal shaped crystal.

(7) *SMART V 4.045 Software for the CCD Detector System*; Bruker AXS Inc.: Madison, WI, 1996.
(8) *SAINT V 4.035 Software for the CCD Detector System*; Bruker AXS Inc.: Madison, WI, 1996.
(9) *SADABS, Program for absorption correction for area detectors*; Bruker AXS Inc.: Madison, WI, 1996.
(10) Sheldrick, G. M. *SHELXS-90, Program for the Solution of Crystal Structure*; University of Göttingen: Germany, 1986.
(11) Sheldrick, G. M. *SHELXL-97, Program for the Refinement of Crystal Structure*; University of Göttingen: Germany, 1997.
(12) *SHELXTL 5.10 (PC-Version), Program library for Structure Solution and Molecular Graphics*; Bruker AXS Inc.: Madison, WI, 1997.

The structure solutions were obtained via the direct methods routine SOLV in the SHELXTL crystallographic package.[14] The hydrogen atoms for the lattice water molecule in **9** were located on the difference Fourier map and their positional and thermal parameters refined.

The structure solution and refinement for all structures was straightforward except for **2** and **2′**. Both compounds grew as very thin slats and larger crystals examined were invariably twinned. Thus it was necessary to collect data on small crystals where the diffracted intensity was marginal, even for a system with a CCD detector. For **2′**, there were two complications encountered in the refinement. First, the structure analysis indicated that crystals of **2′** contained a mixture of Br^- and OH^- anions as lattice counterions. Data were collected on crystals from three different syntheses. The observed fraction of bromide ion roughly ranged from about 0.6 to 0.9 in these three samples. The structure reported in this paper is for the sample with the highest percentage of bromide ion. Because of the nonstoichiometric nature of the counteranions, the structure also indicated a disorder in the location of the lattice water molecules. For this reason, no attempt was made to locate their hydrogen atoms or position them in calculated positions. A further complication arises because of the ambiguity of the space group, *P*2/*c* or *Pc*. The structure reported is for the refinement in the centrosymmetric *P*2/*c* space group. Since it is possible that the observed disorder is due to refinement in the incorrect higher symmetry group, refinement was also pursued in the *Pc* space group. However, it was more difficult to model the disorder, and the refinement led to a higher R_1 value. Hence, it was concluded that the *P*2/*c* refinement provides the best description of the structure at this stage.

The refinement of **2** was also beset by multiple problems. The unit cell initially indexed as orthorhombic with lattice constants of approximately 51.6 × 7.5 × 14.5 Å. Elucidation of a probable orthorhombic space group was ambiguous and initial solution attempts were not successful. Examination of the weighted reciprocal lattice plots clearly indicated a 4-fold superlattice structure parallel to the *a* axis. The recognition of a close match between the *b* and *c* lattice constant of **2** and **2′** suggested a close relation between the two structures and, indeed, it was possible to transform the orthorhombic cell of **2** into a monoclinic lattice with nearly the same values of *b*, *c*, and γ as for **2′** and with a 4-fold multiplication of the *a* lattice constant. Finally, because of this, the compound crystallizes with inherent twinning, given by the twin law matrix

$$[1\ 0\ 2,\ 0\ -1\ 0,\ 0\ 0\ -1]$$

With this assumption, a preliminary refinement of the structure has been obtained which delineates the essential features of the structure. However, at this point, it has not been possible to use appropriate restraints to constrain the anisotropic thermal parameters to be positive definite on al C and N atoms. Further refinement of the structure is planned and will be reported in a specialized journal.

Table 1 summarizes the most important structural and refinement parameters for the 10 compounds. Tables 2 and 3 give the bond distance and angle information for the copper coordination spheres in the various compounds, while Table 4 gives some of the relevant dihedral angles. Full crystallographic details for all structure determinations are available as Supporting Information.

Structure Descriptions

The Copper(I) Complex: [Cu(dmbp)$_2$]Br (1). This compound consists simply of isolated cations and Br^- anions (Figure 1a). The four coordinate Cu(I) cation has distorted tetrahedral geometry. Part of the angular distortion is forced by the "bite" of the bidentate ligand that leads to an average N−Cu−N angle of 80.7(2)°. The Cu−N distances average 2.047(11) Å. The dihedral angle between the two CuN_2 planes is 54.2°. This is probably dictated by the intermolecular forces involving $\pi-\pi$

Table 2. Cu−Ligand Bond Distances

Distance	**1**	**2**	**2′**	**3**	**4**	**4**	**4**	**5**	**6**	**7**	**7**	**8**	**9**
		Cu(1)		Cu(1)	Cu(2)	Cu(1)	Cu(2)	Cu(3)		Cu(1)	Cu(2)		
Cu−N(1)	2.039(5)	2.05(1)	2.085(5)	2.107(9)		1.99(2)			2.05(2)	2.031(4)	1.999(7)		2.026(5)	
Cu−N(1′)	2.057(4)	1.92(1)	1.971(5)	1.988(8)		2.04(2)			2/04(2)				2.038(6)	
Cu−N(11)	2.034(4)	2.02(1)		1.985(8)		2.04(2)								
Cu−N(11′)	2.056(5)	1.93(1)		2.107(9)		1.97(2)								1.981(5)
Cu−O														
Cu−N(ave)	2.046	1.98	2.03	2.05		2.01								
Cu−Br(1)		2.462(2)	2.515(2)	2.400(2)		2.558(4)	2.334(5)		2.394(4)	2.419(1)	2.440(1)	2.474(1)	2.439(1)	2.400(1)
Cu−Br(2)					2.204(2)		2.377(5)	2.438(5)	2.417(4)			2.388(1)	2.635(1)	2.380(1)
Cu−Br(3)/Br(1i)					2.208(2)		2.394(5)	2.492(5)		3.147(1)	3.091)8			2.391(1)
Cu−Br(4)/Br(2i)								2.281(5)				3.256(1)		2.355(1)

(13) *Nicolet Crystallographic Systems User's Guide*, release 81.3; Nicolet X-ray Instruments, 1985.

(14) Sheldrick, G. M. *SHELXTL*, version 5.1; Nicolet X-ray Instruments, 1985.

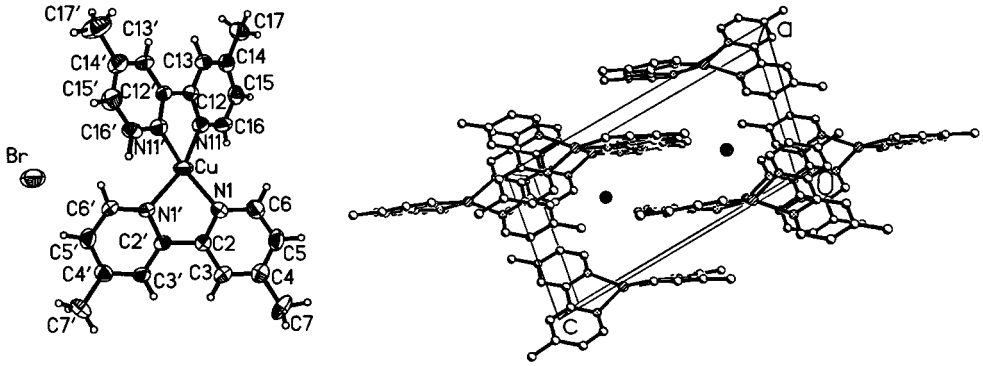

Figure 1. (a) Illustration of the asymmetric unit of **1**, $[Cu(dmbp)_2]Br$. Thermal ellipsoids shown at the 50% probability level. (b) Packing diagram for **1** as viewed down the *b* axis. The large cross-hatched circles are the Br^- ions.

Table 3.

(a) Bond Angles for Compounds **1**−**4**[a]

angle/compound	**1**	**2**	**2**	**2′**	**3**	**4**
		Cu(1)	Cu(2)			
N(1)−Cu−N(1′)	80.8(2)	78.3(5)	78.0(13)	80.4(2)	79.3(3)	81.2(8)
N(11)−Cu−(N11′)	80.6(2)	78.9(5)	84.1(13)		79.1(4)	81.0(7)
N(1)−Cu−N11)	114.1(2)	123.2(5)	102.9(13)	122.7(3)	96.3(1)	101.0(8)
N(1)−Cu−N(11′)	145.5(2)	100.3(5)	121.4(10)	98.3(2)	108.3(3)	178.1(8)
N(1′)−Cu−N(11)	145.2(2)	100.3(5)	174.4(13)		172.4(4)	129.6(8)
N(1′)−Cu−N(11′)	105.2(2)	177.7(5)	90.6(11)	172.2(3)	96.3(3)	97.7(8)
τ		0.91	0.88	0.82	1.07	0.81
N(1)−Cu−Br(1)		118.3(4)	120.6(9)	118.7(1)	120.8(2)	89.2(6)
N(1′)−Cu−Br(1)		91.8(4)	91.3(8)	91.4(2)	92.5(2)	108.7()
N(11)−Cu−Br(1)		118.5(5)	92.9(9)		95.1	121.6(6)
N(11′)−Cu−Br(1)		90.5(4)	116.9(8)		130.9(2)	89.7(6)

(b) Bond Angles for Cu(II) in Compounds **5**−**8**

angle/compound	**5**	**6**	**7**	**8**
N(1)−Cu−N(1′)/N(1i)	80.9(7)	79.6(2)	81.3(4)	80.4(2)
N(1)−Cu−Br(1)	96.0(5)	95.0(1)	96.7(2)	94.3(2)
N(1′)−Cu−Br(2)/Br(1i)	96.2(6)		177.0(2)	98.4(2)
Br(1)−Cu−Br(2)/Br(1i)	97.13(13)	90.69(4)	85.5(1)	104.2(1)
N(1)−Cu−Br(2)/Br(1i)	147.8(7)	173.0(1)		104.5(2)
N(1i)/N(1i)−Cu−Br(1)	159.3(7)			157.4(2)

(c) Copper−Bromine Bond Angles for Compounds **3**, **4**, **7** and **9**

angle/compound	**3**	**4**	**4**	**7**	**9**
		Cu(1)	Cu(2)		
Br(1)−Cu−Br(2)	175.8(1)	125.7(2)		91.20(3)	123.4(1)
Br(1)−Cu−Br(3)/Br(1i)		123.7(2)		93.74(6)	100.9(1)
Br(2)−Cu−Br(3)/Br(1i)		110.7(2)		174.12(5)	102.3(1)
Br(1)−Cu−Br(4)/Br(2i)			105.5(2)		99.8(3)
Br(2)−Cu−Br(4)/Br(2i)			131.2(2)	84.06(4)	101.1(1)
Br(3)−Cu−Br(4)			123.4(2)		130.6(1)

[a] The quantity τ is defined in the text.

Table 4. Dihedral Angles

compound		pyridine ring planes (deg)	CuN_2/CuN_2 planes (deg)	$CuN_2/CuBr_2$ planes (deg)	$CuBr_2/CuBr_2$ planes (deg)	Cu−Br distance (Å)
1	ligand 1/2	8.8/11.5	54.2			
2−Cu(1)	ligand 1/2	1.9/4.1	59.3			2.462
2−Cu(2)	ligand 1/2	4.0/4.0	58.0			2.473
2′		3.4	57.7			2.515
3	ligand 1/2	5.6/4.1	72.0			2.400
4	ligand 1/2	2.2/7.9	51.2			2.550
5		2.2		36.9		
6		5.6		64		
7		4.8		3.1	4.8	
8		2.4		76.7		
9					69.3	

and van der Waals interactions between dmbp ligands. In the structure of **1**, the $Cu(dmbp)_2^+$ and the Br^- ions form interpenetrating pseudo-diamond-like lattices. The ligands composed of N(1) through C(7′) form interdigitated stacks parallel to (1 1 0). The interligand distances alternate between 3.462 and 3.462 Å. In contrast, the pyridine rings of ligands composed of N(11)

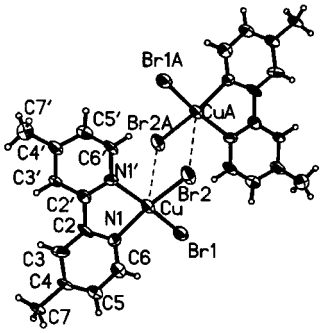

Figure 2. Illustration of the $[(dmbp)CuBr_2]_2$ dimer in **5**. Thermal ellipsoids shown at the 50% probability level.

through C(17′) overlap with pyridine rings of neighboring ligands lying in the (1 0 4) plane, as seen in Figure 1b. This packing is not as efficient with inter-ligand distances alternating between 3.420 and 4.165 Å. In both ligands, a small but significant torsional rotation about the 2,2′ C−C bond is observed, with dihedral angles of 8.8° and 11.5°, respectively, between the planes of two pyridine rings of the bipyridine ligands. Examination of packing diagrams clearly illustrates that this is due to packing forces, so that adjacent pyridine rings remain parallel to each other.

Several comparisons can be made with other $Cu(sbpy)_2^+$ cations.[2d,15] The bite angles are restricted to the 80−82° range by the rigid geometry of the bidentate bipyridine ligand. However, the dihedral angles between the CuN_2 planes show a wide variation. Goodwin et al.[15a] report typical values in the range 60−70°, with distortions from ideal geometry attributed to crystal packing forces. Levy et al.,[2d] however, found a dihedral angle of 89.0° while the other extreme is found in our salt, 54.2°. They also report dihedral angles between the pyridine rings of the sbpy ligands of 2.5 and 15.2°. Our observed values for these dihedral angles are intermediate.

The Mono(dmbp) Cu(II) Complexes: $[(dmbp)CuBr_2]_2$ (5), $(dmbp)CuBr_2$ (6), $(dmbp)Cu_2Br_4$ (7) and $(dmbp)CuBr_2$-(DMSO) (8). These four compounds are each characterized by a single dmbp ligand coordinated to a Cu(II) ion. The first three contain a neutral $(dmbp)CuBr_2$ species as the primary building block. The structure of **5** differs from that of the other two in the extent of connectivity: **5** contains dimer species while **6** and **7** are polymeric. The structures of these latter two are closely related; the former containing stacks of monomers while in the latter dicopper units are the basis of the stacks. Finally, in **8**, the DMSO ligand enters the primary coordination sphere to form a monomeric five-coordinate complex.

(a) $[(dmbp)CuBr_2]$ (5). In this triclinic compound, pairs of $(dmbp)CuBr_2$ species are weakly linked into dimeric molecules around centers of inversion via very long Cu···Br interactions of 3.718 Å, as seen in Figure 2. Because of this interaction, the primary coordination geometry is distorted toward tetrahedral. The trans N−Cu−Br angles are compressed to 148.1° and 159.3° while the dihedral angle between the CuN_2 and $CuBr_2$ planes is 36.9°. The Cu atom is displaced 0.20 Å out of the plane of the bipyridine ligand, trans to the bromide ion.

This weak dimer structure can be compared with that found for a 3,3′-dicarboxylic acid substituted bpy complex.[2e] Here a stronger dimer interaction exists, with the semicoordinated Cu−Br distance now at a more normal value of 3.055 Å and the primary coordination is closer to planar (trans Br−Cu−Br angles of 171.5 and 168.9°). However, this allows the dimers to aggregate in dimer pairs with a second semicoordinate Cu−Br bond formed by one of the copper atoms at 4.014 Å.

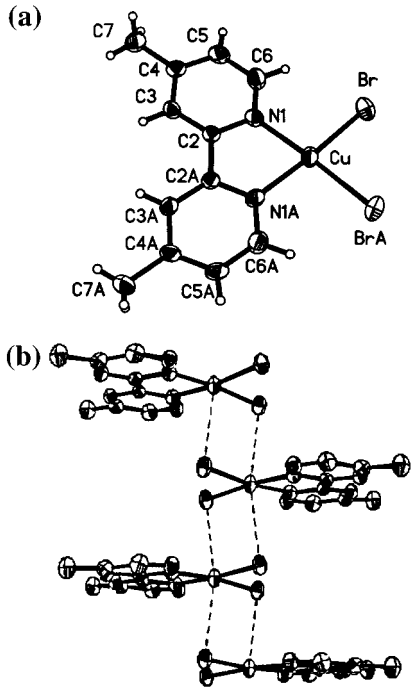

Figure 3. (a) Illustration of the $(dmbp)CuBr_2$ monomer in **6**. (b) Stacking of monomers in **6**. Thermal ellipsoids shown at the 50% probability level.

(b) $(dmbp)CuBr_2$ (6) and $(dmbp)Cu_2Br_4$ (7). Both of these structures have previously been described,[4,16a] although structural details of the latter have not been given.[4] These two monoclinic *C*2/*c* structures are very closely related to each other. In **6**, the Cu(II) ion, which sits on a 2-fold axis, has a cis planar geometry (Figure 3a) with the bidentate dmbp ligand and two bromide ions in the primary coordination sphere. The monoclinic compound is isostructural with $(bpy)CuBr_2$,[16b,2f] which also belongs to the space group *C*2/*c*. The $(dmbp)CuBr_2$ moieties assemble into polymeric stacks through the formation of longer semicoordinate Cu···Br bonds of 3.147(1) Å. This is illustrated in Figure 3b. The repeat pattern seen is that figure is designated a 2(1/2,1/2)(1/2,−1/2) stack in the Geiser notation.[3b] A slight twist in the copper coordination sphere is observed, with the dihedral angle between the CuN_2 and $CuBr_2$ planes of 5.6°. In **7**, a second $CuBr_2$ group is appended to the $(dmbp)CuBr_2$ moiety, forming the planar dimeric unit illustrated in Figure 4a, where the second Cu(II) ion also assumes a nearly planar four-coordinate geometry. Thus the polymeric stacks formed have the same translational symmetry as **6**, as shown in Figure 4b. The semicoordinate bond distances in the dimer stacks are 3.098(1) and 3.256(1) Å.

(c) $(dmbp)CuBr_2$(DMSO) (8). In this compound, a DMSO molecule inserts itself into the copper coordination sphere, yielding a distorted square pyramidal complex. This is illustrated in Figure 5. The nitrogen atoms of dmbp, the oxygen atom from

(15) (a)Goodwin, K. V.; McMillin, D. R.; Robinson, W. R. *Inorg. Chem.* **1986**, *25*, 2033. (b) Munakata, M.; Kitagawa, S.; Ashara, A.; Masuda, H. *Bull. Chem. Soc. Jpn.* **1987**, *60*, 1927. (c) Dobson, J. F.; Green, B. E.; Healy, P. C.; Kennard, C. H. L.; Pukawatchai, C.; White, A. H. *Inorg. Chem.* **1984**, *37*, 649.

(16) (a) Atria, A. M.; Baggio, R.; Garland, M. T.; Gonzalez, O.; Manzur, J.; Pena, O.; Spodine, E. *J. Crystallogr. Spectrosc. Res.* **1993**, *23*, 943. (b) Garland, M. T.; Grandjean, D.; Spdine, E.; Atria, A. M.; Manzur, J. *Acta Crystallogr.* **1988**, *C44*, 1209. (c) Menon, S.; Rajasekharan, M. V.; Tuchagues, J. P. *Inorg. Chem.* **1997**, *36*, 4341.

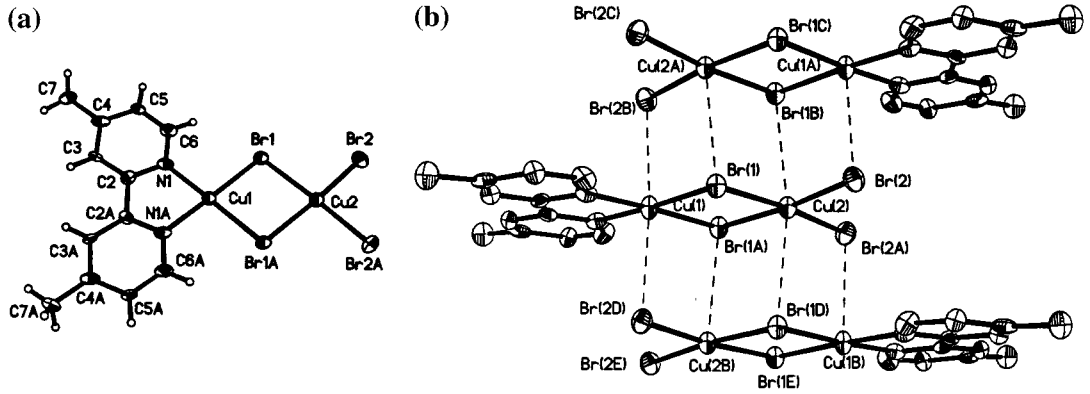

Figure 4. (a) Illustration of the (dmbp)Cu_2Br_4 dinuclear species in **7**. (b) Stacking of the dinuclear units in **7**. The stacks propagate in the *c* direction. Thermal ellipsoids shown at the 50% probability level.

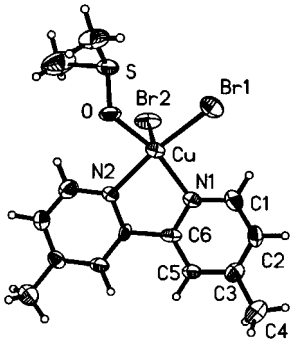

Figure 5. Illustration of the asymmetric unit of **8**, (dmbp)$CuBr_2$-(DMSO). Thermal ellipsoids shown at the 50% probability level.

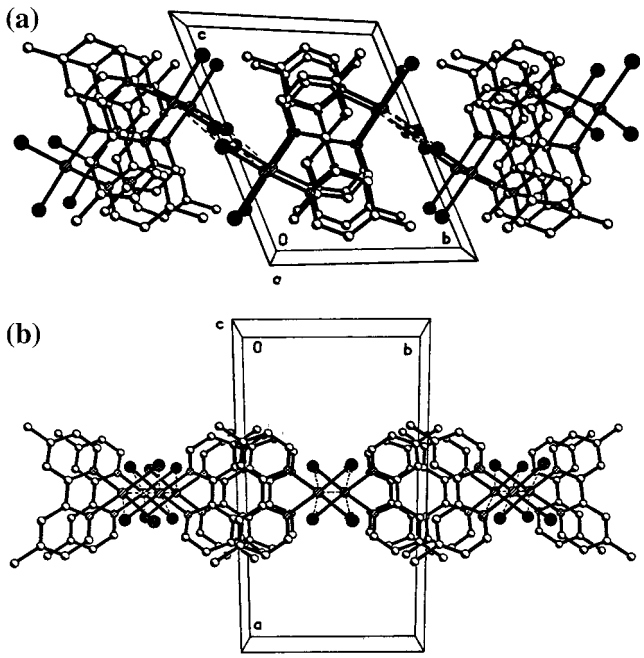

Figure 6. (a) Packing diagram for **5** as viewed from the *a* direction. The *b* axis is horizontal. (b) Packing diagram for **6** as viewed from the *c* direction. The *b* axis is horizontal.

DMSO, and Br(1) form the base of the pyramid with Br(2) occupying the apical site. The apical Cu−Br distance of 2.635-(1) Å is substantially longer than the basal Cu−Br length of 2.439(1) Å, as anticipated for a square pyramidal complex. The trans basal angles are essentially equal, with Br(1)−Cu−N(1′) = 157.4(2)° and N(1)−Cu−O = 157.0(2)°. The dmbp ligands on pairs of adjacent molecules overlap with a distance of 3.53 Å between the planes of the pairs of ligands.

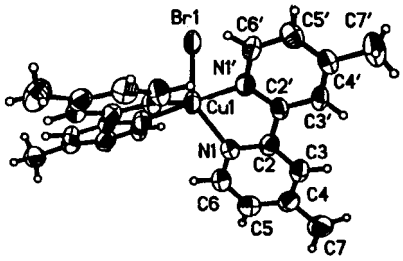

Figure 7. Illustration of the Cu(dmbp)$_2$$Br^+$ cation in **2′**. Thermal ellipsoids shown at the 50% probability level.

A unifying factor in the structures of **5**, **6**, and **7** is the nature of the $\pi-\pi$ stacking interactions that provide the molecular superstructure. All of these three compounds form layered structures through interdigitation of the dmbp ligands, as shown in Figure 6a and b for **5** and **6**, respectively. These figures show the close relationship between the polymorphic structures of **5** and **6** even though the molecular geometries in the two structures appear to be disparate. The uniform $CuBr_2$ chain in **6** distorts via dimerization. Concomitantly, the extent of interdigitation of the dmbp ligands increases. This leads to a shortening of the intermolecular distances within the layer with a large increase in the distance between layers. There is a surprisingly large increase in volume in this process, with the volume per formula unit increasing from 320.25 to 355.55 $Å^3$, an 11% increase. These structural results are consistent with DSC measurements on **6**, which show the onset of a phase transition at ~90 °C (presumably to the **5** structure), followed by thermal degradation above 105 °C. This increase in volume is reflected in a corresponding increase in the distance between the interdigitated dmbp ligands. The distance between the dmbp molecules in **6** is 3.39 Å, while in **5** the distances alternate between 3.67 and 3.77 Å. This leads to an increase in their thermal motion, with the values of U_{eq} in **5** being 50% larger than those in **6**. Similar interdigitation of dmbp ligands occurs in **8**, but this leads to a chain type structure in this case.

It is worthwhile to compare the polymorphism observed for (dmbp)$CuBr_2$ to that observed for the $CuCl_2$(bpy) system,[17] where two polymorphs also exist. One of the polymorphs in the latter system is isomorphous to **6**, in which each Cu atom attains a 4 + 2 geometry through the formation of bibridged stacks. The Cu atoms in the second polymorph, however, have a 4 + 1 coordination through the formation of mono-bridged

(17) (a) Garland, M. T.; Grandjean, D.; Spodine, E.; Atria, A. M.; Manzur, J. *Acta Crystallogr.* **1988**, *C44*, 1209. (b) Hernandez-Molina, M.; Gonzalez-Platas, J.; Ruiz-Perez, C.; Lloret, F.; Julve, M. *Inorg. Chim. Acta* **1999**, *284*, 258.

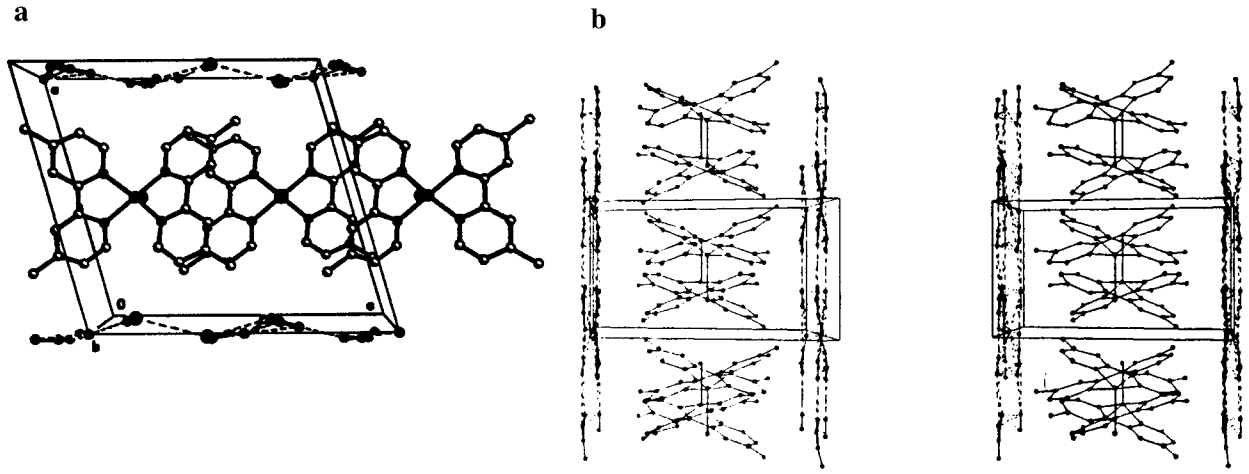

Figure 8. (a) The layered structure in **2′** viewed parallel to the *b* axis. The *c* axis is horizontal. Layers of cations are separated by layers of hydrated bromide and/or hydroxide ions. Thermal ellipsoids shown at the 50% probability level. (b) View of one of the layers, illustrating the interdigitation of the dmbp ligands.

stacks, rather than the dimerization in **5**. A consequence of this stacking pattern is that all of the bpy ligands lie on the same side of the stack. Hence, no interdigitation of ligands occurs. Interconversion between these two polymorphs will be less facile than in the (dmbp)$CuBr_2$ system.

The Bis(dmbp)Cu(II) Complexes: [Cu(dmbp)$_2$Br](OH)·$^1/_2H_2O$ (2) and [Cu(dmbp)$_2$Br](Br/OH)·5$^1/_2H_2O$ (2′). These two closely related compounds are the most enigmatic of this series of compounds. Both compounds are formed under similar conditions and crystals have identical and very characteristic morphologies—very thin slats. The only difference in the crystals of the two compounds is in their optical properties. The OH^- salt, **2**, has a light blue color. In contrast, the mixed Br^-/OH^- salts are nearly opaque when viewed normal to the large face with ordinary light, but are strongly green/brown pleochroic when observed with polarized light (the stronger adsorption occurring when the electric vector is parallel to the long axis of the slat). This similarity carries over the crystal lattice, where, as documented in the Experimental Section, the unit cell of **2** is a 4-fold multiple of the unit cell of **2′**.

The basic building block of both structures is the five-coordinate Cu(dmbp)$_2Br^+$ cation, illustrated in Figure 7 from the structure of **2′**. These cations lie in layers that are parallel to the *bc* plane as seen in Figure 8. Again interdigitation of the dmbp ligand is the driving force for the formation of these layers. The cationic layers are separated by the disordered anionic $[X(H_2O)_{5.5}]_n^{n-}$ layers, where X = Br^- or OH^-. This is illustrated in Figure 8a for **2′**. In both **2** and **2′**, the cations lie on 2-fold axes of rotation that run parallel to the *b* axis, with the Cu and Br atoms lying on these axes. Adjacent layers in **2′** are related by primitive translations parallel to the *a* axis so that the Cu−Br bonds retain the same orientation from one layer to the next for translation parallel to (1 0 0). In contrast, in **2**, the orientation of the Cu−Br bonds assumes a ↑↓↑↓ repeat sequence for translation in that direction, as illustrated in Figure 9.

The Cu(dmbp)$_2Br^+$ cation in **2′** has nearly ideal trigonal pyramidal geometry with the axial N(1′)−Cu−N(1′) angle of 177.2(3)° and the equatorial angles of N(1)−Cu−N(1) = 122.7(3)° and N(1)−Cu−Br = 118.7(1)°. The dihedral angle between the two CuN_2 planes defined by the bidentate ligands is 57.7°. These angular values are typical of other Cu(sbpy)$_2Br^+$ cations.[2f,18]

Figure 9. Illustration of the repeat sequence of Cu(dmbp)$_2Br^+$ ions parallel to the *a* axis in **2**.

Surprisingly, the Cu−Br bond length of 2.515(2) Å is nearly 0.1 Å longer than that of 2.419 Å observed in Cu(bpy)$_2$Br(BF$_4$).[18] The cause of this is not readily apparent, since there are no short hydrogen bonding interactions that might lead to a lengthening of this bond. The Cu−Br bond distances in the OH^- salt, **2**, are intermediate in length (2.463(2) and 2.470(4) Å).

The structural results of **2** and **2′** again clearly demonstrate the major influence the $\pi-\pi$ supramolecular interactions have on dictating the solid-state structures. The layer nature of these two materials was demonstrated in Figure 8a and b gives a view of one of these layers, illustrating how the interdigitation of the dmbp ligands leads to the development of this layer structure. Adjacent cations are related by centers of inversion, so that the planes of the interdigitated dmbp ligands are parallel to each other. The distance between adjacent planes in **2′** is 3.46 Å. The depth of the interdigitation, which is not particularly deep, is such that the C(3)−C(4) type bonds on adjacent ligands are approximately superimposed.

The Mixed Valence Compounds: [Cu(dmbp)$_2$ Br][CuBr$_2$] (3) and Cu(dmbp)$_2$BrCu$_2$Br$_3$ (4). These two compounds contain the copper(II) Cu(dmbp)$_2Br^+$ moiety, similar to those present in **2** and **2′**, cocrystallized with copper(I) bromide species. Compound **3** is an ionic salt consisting of the Cu(dmbp)$_2Br^+$ cations and linear $CuBr_2^-$ anions (Figure 10). In contrast, **4** contains molecular species in which the Br atom on the Cu(dmbp)$_2Br^+$ cation is linked covalently to one of the Cu(I) ions, as illustrated in Figure 11. In this manner a planar bibridged binuclear Cu_2Br_4 unit is developed in which both Cu(I) ions have a trigonal planar geometry.

The Cu(dmbp)$_2Br^+$ cations retain their basic trigonal bipyramidal geometry in both compounds. The major difference is in the length of the Cu−Br bond. The observed distance of 2.400(2) Å in the isolated cation in **3** agrees well with that for the corresponding isolated Cu(bpy)$_2Br^+$ ion in the BF_4^- salt.[18a] The elongation observed in **4** (2.558(4) Å) is consistent with the expectations for a bridged system. Angular distortions from trigonal bipyramidal geometry remain relatively small (Table

(18) (a) Hathaway, B. J.; Murphy, A. *Acta Crystallogr.* **1980**, *B36*, 295. (b) Khan, M. A.; Tuck, D. G. *Acta Crystallogr.* **1981**, *B37*, 1401.

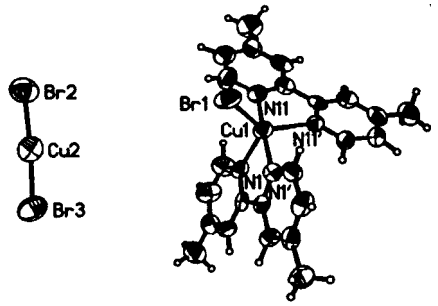

Figure 10. Illustration of the asymmetric unit of the mixed valence $[Cu(II)(dmbp)_2Br](Cu(I)Br_2)$ species in **3**. Thermal ellipsoids shown at the 50% probability level.

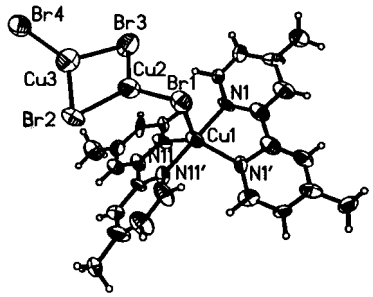

Figure 11. Illustration of the asymmetric unit of the mixed valence $Cu(II)(dmbp)_2BrCu(I)_2Br_2$ species in **4**. Thermal ellipsoids shown at the 50% probability level.

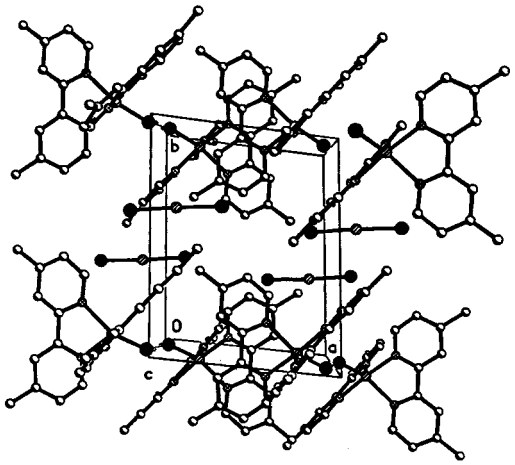

Figure 12. Illustration of the packing in **3** as viewed from the *c* direction. The *b* axis is vertical.

3a). Unusual intermolecular interactions in these two compounds are Br(1)−Br(1) contacts of 3.796 and 3.712 Å, respectively. These distances are substantially shorter than the sum of the Br van der Waals radii (3.9 Å).

Again, the $\pi-\pi$ supramolecular interactions lead to efficient intermolecular packing of the dmbp ligands. In **3**, the $CuBr_2^-$ anions lie in layers roughly at $y = {}^1/_2$, with the cations in layers at $y = 0$. Nevertheless, one set of dmbp ligands, comprised of N(11)−C(17′), is able to form interdigitated stacks parallel to the *b*-axis with a spacing of 3.5 Å. This is illustrated in Figure 12. The nature of the interdigitation alternates within the stack, with interdigitation of the full dmbp ligands within the cationic layers while only single methylpyridine rings stack between the anionic and cationic layers. In contrast, for the other set of dmbp ligands, comprised of N(1)−C(7′), only four are able to stack together in the (101) direction before other set of ligands interrupts the stack. As seen in Figure 13, the molecules in **4** lie in planes parallel to the *ac* plane. Both dmbp ligands form

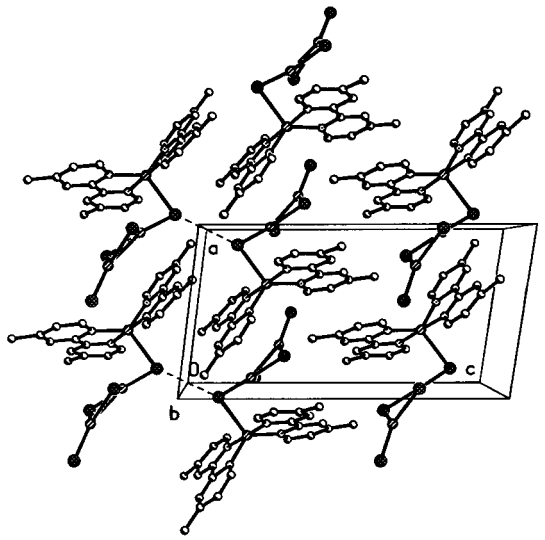

Figure 13. Illustration of the packing in **4** as viewed from the *a* direction. The *c* axis is horizontal.

$\pi-\pi$ dimer pairs with adjacent molecules, with interplanar spacing of 3.63 and 3.55 Å, respectively. The Cu_2Br_3 moieties lie roughly parallel to the dmbp planes, preventing the dmbp ligands from forming infinite stacks.

The isolated $CuBr_2^-$ anion in **3** is nearly linear (Br−Cu−Br = 175.8(1)°) and symmetrical (Cu−Br = 2.204(2) and 2.208-(2) Å). These distances are somewhat shorter than average value of 2.216(10) Å for 12 linear $CuBr_2^-$ anions reported in the Cambridge Structural Database.[19] Only one other structure has a report of shorter Cu−Br distances.[20] This is reasonable, given the lack of any possible hydrogen bonding. The $Cu^I{}_2Br_4$ bibridged species in **4** is essentially planar, with small distortions from trigonal planar geometry for both Cu(I) atoms (Table 3c). For Cu(2), the equatorial angles range from 110.7(2) to 125.7-(2)°, while for Cu(3), the variation is greater, ranging from 105.5(2) to 131.2(2)°. The bridging Cu−Br distances are all longer (2.425 Å(ave.); range 2.377(5) to 2.492(5) Å) than for the terminal Cu−Br distances (2.281(5) and 2.334(5) Å). Despite this, the acute Cu−Br−Cu angles in the moiety (67.9(2)° and 69.0(2)°) yield a short Cu−Cu distance of 2.729(6) Å. These distances and angles are consistent with those found in isolated $Cu_2Br_4^{2-}$ anions.[21] In these previous reports, the bridging Cu−Br distances range from 2.438 to 2.488 Å, the terminal Cu−Br distances vary from 2.239 to 2.334 Å, while the bridging Cu−Br−Cu angles lie between 64.82 and 73.75°.

One noteworthy feature of the structure of **4** is the Cu(II)−Br−Cu(I) bridging angle of only 84.7(2)°. While it is tempting to ascribe this to lone pair localization on the Br^- ion induced by formation of the two Cu−Br bonds, in reality, this is dictated largely by packing forces. This acute angle allows the Cu_2Br_4 moiety to lie nearly parallel to an adjacent dmbp ligand. It is this interaction, which helps prevent the interdigitation of the dmbp ligands. It is interesting to note that the $[Cu(dmbp)_2Br]_2Cu_4$-

(19) Allen, F. H.; Kennard, O. *Chem. Des. Autom. News* **1993**, *8*, 31−37.
(20) (a) Asplund, M.; Jagner, S.; Nilsson, M. *Acta Chem. Scand., Ser. A* **1983**, *37*, 57. (b) Andersson, S.; Hakansson, M.; Jagner, S. *J. Crystallogr. Spectrosc. Res.* **1989**, *19*, 147.
(21) (a) Asplund, M.; Jagner, S. *Acta Chem. Scand. Ser. A* **1984**, *38*, 135. (b) Canty, A. J.; Engelhardt, L. M.; Healy, P. C.; Kildea, J. D.; Minchin, N. J.; White, A. H. *Aust. J. Chem.* **1987**, *40*, 1881. (c) Andersson, S.; Jagner, S. *Acta Chem. Scand. Ser. A* **1987**, *41*, 230. (d) Shibaeva, R. P.; Kaminskii, V. F.; *Kristallografiya* **1981**, *26*, 332. (e) Adams, H.; Candeland, G.; Crane, J. D.; Fenton, D. E.; Smith, A. J. *Chem. Commun.* **1990**, 93.

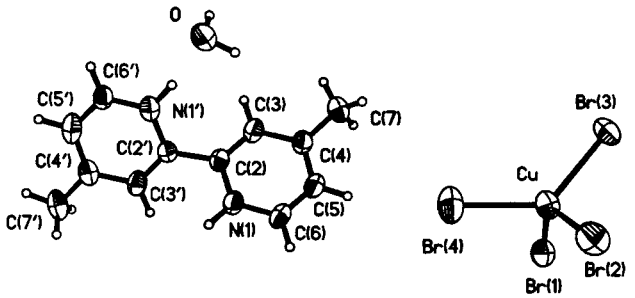

Figure 14. Illustration of the asymmetric unit of **9**, $(dmbpH_2)CuBr_4$. Thermal ellipsoids shown at the 50% probability level.

Br_6 species cited in the Introduction[2f] can be recognized as dimer of the $Cu(dmbp)_2BrCu_2Br_3$ species in **4**.

The $dmbpH_2^+$ Salt: $(dmbpH_2)CuBr_4 \cdot H_2O$ (9). This compound contains the diprotonated dmbp cation and the distorted tetrahedral $CuBr_4^{2-}$ anion (Figure 14). The two pyH^+ rings are now rotated 129.3° about the C(2)−C(2′) bond. The rotation is a balance between electrostatic repulsion between the $N-H^+$ moieties and interactions between the $N-H^+$ group and the C(3)−H group. This torsional angle is substantially less than observed in $bpyH^{2+}$ salts, where they are in the range 152−160°.[22] The crystal packing appears to be more dictated by the electrostatic interactions than $\pi-\pi$ the interactions, with little overlap of the pyridinium rings. A substantial number of structures containing isolated $CuBr_4^{2-}$ anions are known, with 23 cited in the Cambridge Crystallographic Database.[19] With the exception of two TTF-type salts that contain planar anions, the others all have average trans angles between 120 and 140°. A significant feature of the structure is an interspecies contact between Br(1) and Br(4) of 3.941 Å. Contacts of this type have proven to be effective antiferromagnetic superexchange pathways.[23] These contacts should lead to the development of one-dimensional antiferromagnetic behavior.

Discussion

This study clearly demonstrates the wide variety of crystal chemistry that can be obtained through the interaction of an organic ligand with copper halides. In conjunction with the structures of other sbpy complexes with Cu(I) and Cu(II) halides, it is possible to draw several conclusions concerning the nature of the complexes formed. From the mixed valence materials, it is evident that Cu(II)/dmbp complexes are more stable than the corresponding Cu(I)/dmbp complexes. The Cu(I) ion is found to form either the $Cu(dmbp)_2^+$ cation or two- and three-coordinate anionic copper(I) bromide species. With dmbp, the dominant species for copper (II) are clearly the trigonal bipyramidal $Cu(dmbp)_2Br^+$ cation and variations of the $Cu(dmbp)Br_2$ complex. Larger dmbp/Cu(II) ratios favor the formation of compounds containing the $Cu(dmbp)_2Br^+$ species, while excess $CuBr_2$ is able to force the formation of the unusual $(dmbp)Cu_2Br_4$ dimer system.

The stereochemistry of the $Cu(dmbp)_2Br^+$ cations observed in this is close to trigonal bipyramidal. Significantly, this cation does not distort through the formation of additional bonds. It can either stand alone in the lattice, or the bromide ion can bridge to other copper species, as in **4**. The stability of this type of species is confirmed by a survey of the Cambridge Data Base[19] for CuL_2X^+ complexes (L = bpy or *o*-phenanthroline based bidentate ligands) which yielded 137 hits. These species show a range of geometries varying from trigonal bipyramidal to square pyramidal. This has been characterized by the parameter $\tau = (\varphi_1 - \varphi_2)/60$ where φ_1 and φ_2 are the largest and second largest N−Cu−N angles.[24] The value of $\tau = 1$ corresponds to trigonal bipyramidal and $\tau = 0$ to square pyramidal geometry. Typical values lie in the range 0.6−1.0, indicating the trigonal bipyramidal limit is preferred, although a few τ values in the range 0.1−0.2 have been found.[25] For the structure reported here, the τ values range from 0.81 to 1.07 (Table 3a), close to the trigonal bipyramidal limit. These values are in general agreement with those found for a series of Cu(o-phenanthroline)$_2Br^+$ complexes.[25a] In that paper, it is seen that the τ values generally increase for the CuL_2X^+ series in the sequence $\tau(Cl) < \tau(Br) < \tau(I)$. Thus, large X^- species appear to favor trigonal bipyramidal stereochemistry.

In contrast, the four coordinate $Cu(dmbp)Br_2$ species is extremely susceptible to expansion of its coordination sphere. In this study, the Cu(II) ion attains a 4 + 1 coordination geometry in **5**, 4+2 geometry in **6** and **7**, and square pyramidal geometry in **8**. Again, the crystallographic literature is rife with examples of $CuLX_2$ species that aggregate into dimers, stacks etc through expansion of the coordination geometry to 4 + 1 or 4 + 2. A detailed analysis of the geometries of these types of system would be a useful chapter in the analysis of the stereochemistry of Cu(II) complexes.

Distorted tetrahedral coordination geometry was observed in this study for both the $Cu(dmbp)_2^+$ species and the $CuBr_4^{2-}$ species. Both show distortions from ideal tetrahedral geometry. The distortions observed are consistent with the detailed analysis performed by Raithly et al.[26a] on four coordinate Cu(I) and Cu(II) complexes. For the bis bidentate ligand complexes, as in $Cu(dmbp)_2^+$, they attribute the observed deviations between the planes of the bidentate ligands from the ideal 90° angle to packing forces. The stacking interactions observed in this study certainly support this conclusion. For the $CuBr_4^{2-}$ cations, the distortions have been shown to occur predominately along the D_{2d} distortion pathway for the D_{4h} to T_d transformation.[26b]

Despite the wide variety of structural chemistry exhibited in this study, it comes short of demonstrating all of the possible structural varieties. For example, bpy forms a hydroxy-bridged dimer with copper(II) bromide[2f] rather than the $[Cu(dmbp)_2Br^+]$-$OH \cdot 6^1/_2H_2O$ salt found in this study. A bibridged $[Cu(bpy)Br]_2$ dimer has been reported, with bridging Br atoms.[27] More recently, a bibridged $[Cu(bpy)(CuCl_2)]_2$ dimer has been reported in which the bridging species are linear $CuCl_2^-$ anions.[28] In addition, the copper(I) bromide species can take on four-coordinate geometry and assemble into extended structures.[29,2f]

(22) (a) Ma, G.; Ilyukhin, A.; Glaser, J. *Acta Crystallogr.* **2000**, *C56*, 1473. (b) Troyanov, S. I.; Rybakov, V. B.; Mazo, G. N.; Il'inskii, A. L. *Zh. Strukt. Khim.* **1989**, *30*, 193.

(23) (a) Albrecht, A. S.; Landee, C. P.; Sanic, Z.; Turnbull, M. M. *Mol. Cryst. Liq. Cryst.* **1997**, *305*, 333. (b) Hammar, P. R.; Dender, D. C.; Reich, K. H.; Albrecht, A. S.; Landee, C. P. *J. Appl. Phys.* **1997**, *81*, 4615.

(24) (a) Harrison, W. D.; Kennedy, D. M.; Ray, N. J.; Sheahan, R.; Hathaway, B. J. *J. Chem. Soc., Dalton Trans.* **1981**, 1556. (b) Nagle, P.; O'Sullivan, E.; Hathaway, B. J.; Muller, E. J. *Chem. Soc., Dalton Trans.* **1990**, 3399. (c) Addison, A. W.; Rao, T. N.; Reedijk, J.; van Rijn, J.; Vershoor, G. C. *J. Chem. Soc., Dalton Trans.* **1984**, 1349.

(25) (a) Murphy, G.; O'Sullivan, C.; Murphy, B.; Hathaway, B. *Inorg. Chem.* **1998**, *37*, 240. (b) Bush, P. M.; Whitehead, J. P.; Pink, C. C.; Gramm, E. C.; Eglin, J. L.; Watton, S. P.; Pence, L. E. *Inorg. Chem.* **2001**, *40*, 1871. (c) Potocnak, I.; Dunaj-Jurco, M.; Miklos, D.; Massa, W.; Jager, L. *Acta Crystallogr.* **2001**, *C57*, 363.

(26) (a) Raithby, P. R.; Shields, G. P.; Allen, F. H.; Motherwell, W. D. S. *Acta Crystallogr.* **2000**, *B56*, 444. (b) Keinan, S.; Avnir, D. *J. Chem. Soc., Dalton Trans.* **2001**, 941.

(27) Healy, P. C.; Pakawatchai, C.; White, A. H. *J. Chem. Soc., Dalton Trans.* **1985**, 2531.

(28) Cui, Y.; Chen, J.; Chen, G.; Ren, J.; Yu, W.; Qian, Y. *Acta Crystallogr.* **2001**, *C57*, 349.

(29) Subramanian, L.; Hoffmann, R. *Inorg. Chem.* **1992**, *31*, 1021.

One of the common structural themes in these structures are the intermolecular $\pi-\pi$ stacking interactions between the dmbp ligands. It is probable that in the mixed valence species, for example, the optimization of these interactions determine whether the copper(I) bromide species forms isolated anions (**3**) or are bridged to the $Cu(dmbp)_2Br^+$ species(**4**). It is clearly these interactions that stabilize the layer structure in **2** and **2′**, as well as in **5**, **6**, and **7**. Thus the structural chemistry of copper/sbpy complexes will be very dependent upon the nature of the substituents appended to the bpy ligand. This is evident in the examination of $Cu(sbpy)_2^+$ structures[15] where the dihedral angle between the two bpy planes varies from the nearly ideal tetrahedral value of 90° to the minimal value of 54.2° observed in this study. While the $\pi-\pi$ interactions are extremely important in the determination of the solid state structures in these systems, they are not unusually strong. For example, in the silver(I) dipyridyl ketone complexes, the inter-ring distances are in the range 3.12−3.20 Å, compared to the 3.4−3.7 Å observed in these structures.

One intriguing question that is raised in this study is the source of the variation of Cu−Br bond lengths in the $Cu(sbpy)_2Br^+$ species. Comparison of the values observed for the two mixed valence compounds strongly suggest that this distance is influenced by the formation of a bridging Cu(II)−Br−Cu(I) interaction (2.400(2) Å for **3** vs 2.558(4) Å for **4**). However, the distances in **2** and **2′** are intermediate in value (2.47(ave.) Å in **2** and 2.515(2) Å in **2′**) and there are no strong hydrogen bonding interactions evident in those structures to explain the elongation. Examination of Table 4 reveals an interesting correlation between the Cu−Br distance and the dihedral angle between the dmbp ligands coordinated to the copper ion. It is seen that the larger the dihedral angle, the shorter the Cu−Br bond. This correlation extends to the other $Cu(sbpy)_2Br^+$ species reported in the literature.[4f,17] This is logical since interligand repulsions between the C(6) and C(6′) hydrogen atoms force the dmbp ligands to twist away from an eclipsed configuration. The longer the Cu−Br distance, the more space that will exist for this twist. In addition, given the importance of the $\pi-\pi$ discussed above, it is likely that the observed Cu−Br distances represent a balance between these $\pi-\pi$ interactions and interspecies interactions involving the bromide ion.

Another lesson reiterated in this and other studies is that the solid-state structure cannot be predicted from the stoichiometry. An example of this are the four compounds $Cu(dmbp)_2Cu_2Br_4$ (**4**), $[Cu(bpy)_2]Cu_4Br_8]$,[2f] $Cu(bpy)_2Cu_2Cl_4$[30] and $Cu(en)_2Cu_2Br_4$,[2g] which all have the same stoichiometry. Nevertheless, the structures all exhibit different connectivities in the crystalline state. In **4**, the Cu(II) ion is coordinate by one of the Br atoms from the nearly planar bibridged $Cu_2Br_4^{2-}$ species. In the bpy complex, the Cu(I)/Br moiety has aggregated into a stair step tetramer. The two $Cu(bpy)_2^{2+}$ fragments coordinate to terminal Br atoms of the resultant $Cu_4Br_8^{4-}$ oligomer. The $Cu(bpy)_2Cu_2Cl_4$ structure is very intriguing, containing both isolated linear $CuCl_2^-$ anions and Cu(I) chloride chains decorated with $Cu(bpy)_2$ moieties. The Cu(I) chains have stoichiometry $\{[Cu(bpy)_2]_2(Cu_2Cl_6)Cu\}_n^{n-}$ are built up from Cu_2Cl_6 dimeric units formed by edge sharing two $CuCl_4$ tetrahedra. The Cu_2Cl_6 synthon units are linked into chains by Cu(I) ions and capped by the $Cu(bpy)_2^{2+}$ species. In all three of these cases, the Cu(II) ion has a distorted trigonal bipyramidal stereochemistry. In contrast, for the en system, the Cu(I)/Br subsystem now forms infinite $(CuBr_2)_n^{n-}$ chains of edge-shared tetrahedra. Without terminal halide ions, the $Cu(en)_2^{2+}$ species now can only form semicoordinate Cu···Br bonds to the bridging bromide ions in the chain. Thus it attains a 4 + 2 elongated octahedral stereochemistry in contrast to the other two.

Finally, it should be stated that any extrapolation of the structural chemistry present in the solid state to what is present in solution is extremely tenuous, especially concerning extended interactions. The lability of the Cu(II) coordination sphere for mondentate ligands means that it is likely that the $Cu(dmbp)Br_2$ species undergoes at least partial dissociation in solution. The stability of the $Cu(sbpy)_2Br^+$ cations are probably sufficient for its retention in solution, as supported by the recent EXAFS study of copper/bpy in styrene solutions.[31] However, their suggestion of a $Cu(II)Br_3^-$ species does not seem reasonable. While compounds with that stoichiometry are known, they always aggregate in the solid state so that the Cu(II) ion attains a higher coordination number.

Acknowledgment. The use of the Single Crystal Diffraction Facility at the University of Idaho is gratefully acknowledged. The work was supported in part by ACS-PRF 34779-AC5.

Supporting Information Available: For compounds **1**−**7**, seven X-ray crystallographic files, in CIF format; for compounds **8** and **9**, tables listing data collection and refinement details atomic positions and equivalent isotropic thermal parameters, bond distances and angles, anisotropic thermal parameters, and hydrogen atom positions. This material is available free of charge via the Internet at http://pubs.acs.org.

IC010229V

(30) Kaiser, J.; Brauer, G.; Schröder, F. A. *J. Chem. Soc., Dalton Trans.* **1974**, 1490.

(31) Kickelbick, G.; Reinohl, U.; Ertel, T. S.; Weber, A.; Bertagnolli, H.; Matyjaszewski, K. *Inorg. Chem.* **2001**, *40*, 6.